SCA2003-63: SPONTANEOUS IMBIBITION IN LOW PERMEABILITY CARBONATES

Can Ulas Hatiboglu, Ugur Karaaslan and Serhat Akin
Department of Petroleum and Natural Gas Engineering
Middle East Technical University
06531, Ankara, Turkey

This paper was prepared for presentation at the International Symposium of the Society of Core Analysts held in Pau, France, 21-24 September 2003

ABSTRACT
Spontaneous imbibition is important in oil recovery from fractured and low permeability tight gas reservoirs. Gas-water spontaneous imbibition experiments were conducted using low permeability heterogeneous limestone core plugs. The interfacial tension was changed by adding differing amounts of alcohol to water. It was observed that the true residual saturation of gas is very small for all cases. A much larger pseudo-residual saturation was achieved early in the imbibition stage but gas continued to be produced at extremely low rates until the true saturation was reached. The gas-water spontaneous imbibition performance was modeled using a mathematical model where the porous medium is represented as a bundle of equal but tortuous capillary tubes. Input data for this model was obtained from serial thin sections using a state of the art image processing system and a computerized microscope. The gaps between the thin sections were constructed using geostatistical techniques. It was observed that the model successfully explained the imbibition process in samples where pores with varying circularity were present. Average number of pore throats meeting at one pore in the pore skeleton (coordination number) was less than six for all cases.

INTRODUCTION
Spontaneous imbibition is perhaps the most important phenomenon in oil recovery from fractured reservoirs. For such reservoirs the rate of mass transfer between the rock matrix and fractures usually determines the oil production [1]. Imbibition is also essential in evaluation of the rock wettability [2]. For spontaneous imbibition, the main driving force is capillary suction. Because of the strong capillary forces, the smallest pore bodies which are next to the interface are usually invaded first. The displacement takes place at small but finite capillary numbers [3]. The rate of imbibition is usually a function of porous media and fluid properties such as absolute and relative permeability, viscosity, interfacial tension, and wettability [4]. Most experimental work on imbibition behavior has concentrated on the scaling aspects of the process in order to estimate oil recovery from reservoir matrix blocks that have shapes, and sizes different from those of the laboratory core samples [5].

In mathematical modeling of imbibition, two approaches are practiced. The first approach uses a sugar-cube type matrix-fracture system proposed by Warren and Root [1] where the communication occurs at the matrix-fracture interface [6]. The second approach is based on a representative elemental volume averaged fracture-matrix system [5, 7]. Both approaches use empirically determined mass transfer functions.

Kazemi et al. [6] presented numerical and analytical solutions of oil recovery using empirical, exponential transfer functions based on the data given by Aronofsky et al. [8] and Mattax and Kyte [9]. They proposed a shape factor that included the effect of size, shape, and boundary conditions of the matrix. Later, this shape factor was generalized by Ma et al. [10] to account for the effect of viscosity ratio, sample shape, and boundary conditions. They proposed the following equation:

$$t_D = t\sqrt{\frac{k}{f}}\frac{s}{m_s L_c^2} \qquad m_s = \sqrt{m_w m_{nw}} \tag{1}$$

To date, much of the focus on imbibition has centered on carbonaceous rocks. This is a result of the importance of the North Sea Chalks [11], the California Diatomites [12], the West Texas Carbonates [13], and the Middle Eastern Limestones. Even though the literature is vast on recovery of oil by water imbibition, the number of studies conducted on imbibition in tight gas reservoirs is limited [14]. This study presents basic core analysis data and the results obtained from experimental spontaneous imbibition in low permeability vugular and fractured limestone samples. The imbibition data is scaled via the equation proposed by Ma et al. [10]. The gas-water spontaneous imbibition performance was modeled using a mathematical model where the porous medium is represented as a bundle of equal but tortuous capillary tubes. Input data for this model was obtained from serial thin sections (three per zone) taken from the top, middle and the bottom of the core plugs using a state of the art image processing system and a computerized microscope. The gaps between the thin sections were constructed using 3D kriging.

EXPERIMENTAL EQUIPMENT AND PROCEDURE

Experiments were performed with 3 limestone core plugs obtained from different wells in a carbonate field located in Southeast Turkey using distilled water and alcohol with concentrations of 20% and 40% alcohol by volume. The rock samples were cylindrical with a length of 2.88cm and a radius of 1.27cm with varying porosities and permeabilities (Table 1). The cores were sealed with epoxy on the sides parallel to the flow direction to obtain one-dimensional imbibition. Each sample core was suspended by means of a Plexiglass and steel frame directly from a weighing balance in an acrylic container filled with water was connected to a water reservoir leveled to bottom of the core plug. This ensured to eliminate evaporation effects. The core weight measurements were recorded by a personal computer. After the experiments, the cores were dried in an oven and thin sections were collected from top, middle and bottom of each core. Color images of the thin sections were captured using a camcorder connected to a personal computer. Using a servo controlled tray mechanism [15] multiple images that cover the whole section were acquired from these thin sections which then were analyzed using an image processing software at a magnification level of 40X. Finally the images were converted to 8-bit grayscale and binary forms respectively. These images formed a single wide, high resolution image (between 3200x5040 pixels and 4480x5760 pixels) of the corresponding thin section. Porosity, pore size distribution, and circularity of the core plugs were then obtained.

Table 1 Permeability and porosity of the limestone core plugs.

Plug	5				9				14			
Thin Section	1	2	3	Helium	1	2	3	Helium	1	2	3	Helium
ϕ, fraction	0.28	0.27	0.22	0.22	0.23	0.34	0.27	0.23	0.27	0.27	0.24	0.27
k_l, md	4.6				0.1				116			

RESULTS

The weight gain data collected from imbibition experiments are expressed in terms of dimensionless time versus recovery plots (Fig. 1) using Eq.1. Repeatability of the experiments was checked using water as the imbibing fluid in core plug #9. An error of maximum 0.5% was observed (Fig. 1a). None of the core plugs showed similar characteristics in the imbibition plot. The differences in permeability of the samples affect the duration of imbibition Visual observations indicated that the lowest permeable core plug, #9 contained more non-circular vugs that are probably not interconnected to each other. An S-shaped imbibition recovery curve was obtianed for this sample. The highest permeable limestone, #14 on the other hand deviated enormously from the expected line of curvature showing a possible heterogenity effect. Image analysis of thin sections revealed tiny hair like vertical fractures providing pathways for faster imbibition. Less permeable matrix continued to imbibe and this resulted in a change in the recovery curve observed as a slope change. For the remaining time slope was again the same. In general, thin section analysis of both core plugs showed similar pore characteristics. Seven different pore types were identified from the image analysis. Approximately 50% of core plug #9 was dominated by pores sized 10 μ and less, which probably served as a fine screen that resulted in low permeability. Core plug #5 was more concentric around 20 μ sized pores, and low on 10 μ sized ones (Fig. 2).

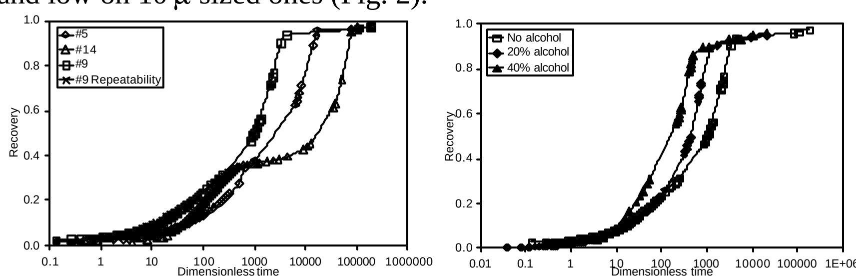

(a) (b)

Figure 1: Imbibition plots for different core plugs (a) and different imbib ing fluids (b).

The interfacial tension was changed by adding differing amounts of alcohol to water (Fig. 1b). As the interfacial tension was lowered the amount of fluid imbibed has increased. This is expected since addition of alcohol decreases the density. There are several phenomena taking place including changes in capillary forces, buoyancy forces and the dimensionless time; much better analysis is required. Moreover, the square root viscosity product in Eq. 1 increases that in turn decreases the dimensionless time. The addition of alcohol to the limestone core plugs might have created a partial wetting effect.

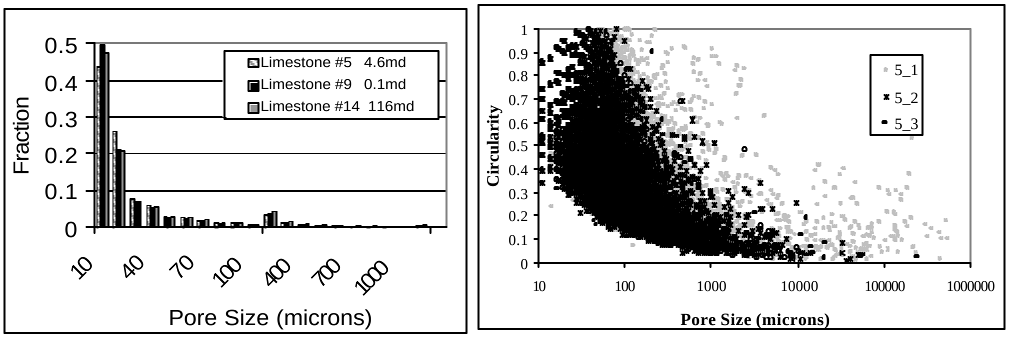

Figure 2 Pore size distribution (left) and circularity (core plug #5) plots (right).

Another interesting aspect of these experiments was the very low trapped gas saturation. The strong capillary forces and the small pore throat to body aspect ratio [15] of the carbonates analyzed here suggests much snap-off and trapped gas. However, for snap-off to occur, pore corners and crevices must fill with wetting liquid and sufficient liquid for snap-off must accumulate at pore throats before the pore is filled completely by the advancing imbibition front. It could be speculated that trapped gas saturation was low because the advancing front fills pores with water (bulk flow) at least as rapidly as pore corners fill with water (film flow). Indeed, recent pore-level network modeling of imbibition shows that in the absence of flow in pore corners the displacement pattern is a flat front with little or no trapping of the nonwetting phase [16].

In order to relate imbibition rates to pore structure, effective medium approximation (EMA) that has been previously used to predict the electric, hydraulic conductance and also permeability was used. For straight cylindrical throats of length *y* and circular cross-section of radius *r*, the hydraulic conductance, g is given by, $pr^4/8y$ [17]. As a criterion to fix effective conductance, g_{eff} it was required that the incremental pressure changes induced when the individual conductances g_i were replaced by g_{eff} in this medium should average to zero. A throat channel with radius r_i in the heterogeneous pore structure was replaced by a throat with radius r_{eff}. The self consistency condition could be used to obtain r_{eff} as the solution of the following implicit equation:

$$\sum_{i=1}^{N} \frac{g_{eff}(r_{eff}) - g_i(r_i)}{g_i(r_i) + [(z/2)-1]g_{eff}(r_{eff})} = 0 \tag{2}$$

where *z* is the spatial average coordination number that is defined as the average number of branches meeting at one node in the skeleton. Using a generalized reduced gradient method for finding the zero of a function, Eq. 2 can be solved for the g_{eff}, thereby obtaining the characteristic throat radius r_{eff}. Using r_{eff} the water adsorption coefficient, *C* which is essentially equivalent to sorptivity parameter in soil physics, may then be obtained using the following equation [18]:

$$C = f\, r \sqrt{\frac{rgd \cos q}{2mt}} \tag{3}$$

where ϕ is porosity, ρ is density, γ is interfacial tension, μ is the viscosity of the fluid, *q* is the contact angle, δ is the pore shape factor defined as the deviation from circularity of the cross-section of the haydraulic radius, τ is turtuosity which was assumed to be equal to 3 [18]. The capillary imbibition kinetics shows two parts: a first part that define water adsorption, and a second part defining the saturation. The slope of the curve during water adsorption is the water adsorption coefficient *C*. Since pore shape plays an important role on imbibition performance, a further improvement on predicting throat radius was made by dividing the areas by circularity since a tubular would be less efficient than elongated cross-sections. Finally, the missing radius and circularity data was obtained by 3D kriging [19] .

Effective radius and water adsorption coefficient values obtained using Eq. 2 and 3 for different coordination numbers and different thin sections are given in Table 2 and plotted in Fig. 3. Due to the heterogeneous nature of the core plugs different values were observed at different parts of the core plugs. When z=2, the effective radius reaches the lowest value in comparison with mean radius for all core plugs. This is due to the fact that r_{eff}, which has been defined from the throat size distribution and the spatial average coordination number, is not a real radius of the rock pores but rather it is a statistical effective radius. Therefore the effective hydraulic radius not only contains information on the effective pore space but also the topology of the fluid flow. On the other hand, when the coordination number is high (i.e. 100) or 8 the effective radius reaches the highest value and the adsorbed water per unit area increases. The calculated water adsorption coefficients for z=6 and z=12 are much closer to the experimental data then are the z=2 and z=100 values. This implies that capillary imbibition takes place essentially in more than one dimension and the flow has a 3-D character. In samples with more connectivity between the throats an increase of coordination number has been observed. Stand alone analyses of the thin sections also show that different parts of the core plugs show different imbibition characteristics. This in accord with the heterogeneous nature of the core plugs. When kriged data is used the results improved significantly. This is expected as kriging provides a smooth change between low connectivity and high connectivity regions. The addition of alcohol on the other hand clearly reduces the adsorbed water. As the amount of alcohol increases the interfacial tension decreases and the effective pore throat radius decreases. This effect can be attributed to partial wetting effects.

Conclusions

Gas-water with and without alcohol spontaneous imbibition experiments were conducted using heterogeneous limestone core plugs. It was observed that the true residual saturation of gas is very small for cases where water and water with alcohol imbibed. Thin section analysis of both core plugs showed similar pore characteristics and seven different pore types were identified. The mathematical model developed using EMA approach successfully explained the imbibition process in samples where pores with varying circularity were present but had difficulty in a core plug where hairline fractures were present. Average number of pore throats meeting at one pore in the pore skeleton (coordination number) was more than six showing 3-D character for all cases.

Table 2 Water Adsorption Coefficient Comparison

z\C	5_1	5_2	5_3	9_1	9_2	9_3	14_1	14_2	14_3
2	1.45	0.7	0.59	1.59	0.95	0.73	0.76	0.74	0.63
6	2.17	1.26	1.11	1.16	2.2	1.46	1.89	1.63	1.2
12	2.86	1.73	1.51	1.59	3.18	2.04	2.86	2.36	1.63
100	7.14	4.29	3.09	3.66	8.32	5.11	7.66	6.36	3.93
z\ r_{eff}									
2	6.93	1.88	2.04	2.23	2.45	2.13	2.52	2.31	1.97
6	10.37	3.38	3.85	1.63	5.67	4.26	6.26	5.08	3.74
12	13.67	4.65	5.23	2.23	8.19	5.95	9.48	7.35	5.09
100	44.99	15.82	14.57	7.05	30.97	20.81	38.41	28.69	16.65

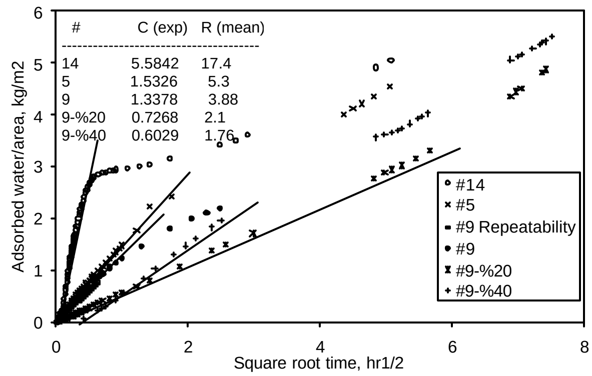

Figure 3 Experimental water adsorption coefficient plot.

References

1. Warren J.E., Root P.J.: “The Behavior of Naturally Fractured Reservoirs,” SPE Journal, 245-255, Sept. 1963.
2. Morrow N.R., Ma S., Zhou X., Zhang X.: “Characterization of Wettability from Spontaneous Imbibition Measurements,” CIM 94-475, 45th Ann.Tech. M. 1994..
3. Sahimi M. “Flow and Transport in Porous Media and Fractured Rock: From Classical Methods to Modern Approaches”, VCH, Weinheim, Germany, 1995, 482 pp.
4. Zhang X., Morrow N.R., and Ma S.: “Experimental Verification of a Modified Scaling Group for Spontaneous Imbibition,” SPERE, Nov. 1996, 280-285.
5. De Swaan A.: “Theory of Waterflooding in Fractured Reservoirs,” SPEJ, 117-122, April 1978.
6. Kazemi H., Gilman J.R., El-Sharkaway A.M.: “Analytical and Numerical Solution of Oil Recovery From Fractured Reservoirs Using Empirical Transfer Functions,” SPE 19849, SPE 64th Ann. Tech. Conf., San Antonio, TX, Oct. 8-11, 1989, 827-842.
7. Civan F.: “A Theoretically Derived Transfer Function for Oil Recovery From Naturally Fractured Reservoirs by Waterflooding,” SPE 27745 SPE/DOE 9th Symp. Imp. Oil Rec., Tulsa, Oklahoma, April 17-20, 1994.
8. Aranofsky J.S, Masse L., Natanson S.G.: “A Model for the Mechanism of Oil Recovery from the Porous Matrix Due to Water Invasion in Fractured Reservoirs,” Trans. AIME, 213, pp 17, 1958.
9. Mattax C.C., Kyte J.R.: “Imbibition Oil Recovery From Fractured, Water-Drive Reservoirs,” SPE Journal 177-184, June 1962, Trans. AIME, 225.
10. Ma S., Morrow N.R., Zhang X., “Generalized Scaling of Spontaneous Imbibition Data for Strongly Water Wet Systems” CIM 95-138, 6th Pet. Conf. Canada, (1995).
11. Cuiec L., Bourbiaux B., Kalaydjian F.: “Oil Recovery by Imbibition in Low-Permeability Chalk,” SPE Formation Evaluation Sept. 1994, 200-208.
12. Akin S., Schembre J.M., Bhat S.K., ve Kovscek A.R.: “Spontaneous Imbibition Chracteristics of Diatomite” J. Pet. Sci. Eng., (25), 3-4, 149-165, 2000.
13. Schechter D.S., Guo, B., “An integrated investigation for Design of a CO_2 Pilot in the Naturally Fractured Spraberry Trend Area, West Texas,” SPE 39881, 1998 Int. Pet. Conf., Villahermosa, Mexico, March 3-5, (1998).
14. Kantzas A., Pow M., and Allsopp, K., "Co-current and Counter-current Imbibition Analysis for Tight Fractured Carbonate Gas Reservoirs", CIM paper 97-181, presented at the 7th Saskatchewan Petroleum Conference, held in Regina Saskatchewan, October 20-22, 1997..

15. Hatipoglu C.U., “Automated Porosity Measurement Using Image Analysis Techniques” Msc Thesis, Middle East Technical University, 2002.
16. Blunt, M.J., Scher, H.J., 1995. “Pore-level modeling of wetting”. Phys. Rev. E: Stat. Phys., Plasmas, Fluids, Relat. Interdiscip. Top. 52 6 , 6387–6403.
17. Doyen P. M., “Permeability, conductivity and pore geometry of sandstone”, J. Geophys. Res., Vol.93, pp.7729-7740, (1988)
18. Benavente D., Lock P., Cura M.A.G.D., Ordonez S., “Predicting the Capillary Imbibition of Porous Rocks from Microstructure” Trans. Por. Med. 49, 59-76, (2002).
19. Deutsch, C. V. and Journel A.G., “GSLIB: Geostatistical Software Library and User's Guide (Applied Geostatistics Serie s)” Oxford University Press, 369 pp, 1997.